ROBUST VIDEO WATERMARKING USING MAXIMUM LIKELIHOOD DECODER

Abolfazl Diyanat[1,2]*, Mohammad Ali Akhaee*[1]*, and Shahrokh Ghaemmaghami*[1,2]

Department of Electrical Engineering[1] and Electronics Research Institute[2] Sharif University of Technology
Tehran, Iran
email: diyanat@ee.sharif.edu, akhaiee@yahoo.com, ghaemmag@sharif.edu

ABSTRACT

In this paper, a robust multiplicative video watermarking scheme is presented. We segment the video signal into 3-D blocks like cubes, and then apply 3-D wavelet transform to each block. The watermark is inserted through multiplying the low frequency wavelet coefficients by a constant parameter that controls the power of the watermark. The proposed watermark extraction procedure is based on the maximum likelihood rule applied to the watermarked wavelet coefficients.

1. INTRODUCTION

Multimedia watermarking has been proposed as an elegant solution to the problem of copyright protection. However, there are several other applications for watermarking, such as broadcast monitoring, fingerprinting, authentication, etc. [1]. Among the media signals, image and video signals have been found to be of more concern for watermarking, due to fast growing demand for capturing such media in new handsets and transmitting them over the web. In this paper, we extend the idea behind the image watermarking algorithms introduced in [2, 3] to the problem of video watermarking.

Video is a moving picture signal in nature, so methods for watermarking of still image may actually be extended to video watermarking by minimal effort. However, this extension is technically rejected for certain reasons, as: i) a video signal generally contains sequences of highly correlated frames, ii) there exist some attacks applicable just for video signals such as MPEG compression, spatial desynchronisation, frame collision, etc., and iii) video signals often deal with real-time applications, hence the use of real-time watermarking methods could specifically be essential in cases of video [4].

There exist several video watermarking algorithms that embed watermark in compressed domain [5, 6]. For example, *Belhaj* in [5] embeds watermark in the MPEG-4 format based on QIM (quantization index modulation) scheme considering perceptual masking. *Langelaar* et al. [6] proposed two methods for embedding the message bits directly into an MPEG compressed video bitstream. The first technique watermarks the signal by changing the variable length codes in the bitstream, while the other one discards some of the high frequency DCT coefficients of the bitstream for data hiding. These watermarking algorithms are suitable for real-time video applications. However, these methods are restricted to a specific video compression standard.

Another class of video watermarking systems use spatial domain [7, 8] or transformed domains such as discrete wavelet transform (DWT) [9], discrete Fourier transform (DFT) [10] and DCT [11] for data embedding. These techniques that are applied in uncompressed domains, must be robust to the compression attacks. Our proposed method falls into this category.

Among image and video watermarking methods, several schemes use wavelet transform. *Chan* and *Lyu* embed different parts of a single watermark into different scenes of a video using wavelet transform. Watermark is embedded into video frames by changing position of some DWT coefficients according to specific rules [12]. *Guo-juan* in [13] proposes a blind video watermarking based on combination of Zernike moments and singular value decomposition (SVD). Here, the SVD is applied to approximation coefficients and the maximum singular value is used for data hiding.

Watermarking systems can be categorized into additive and non-additive methods based on the embedding rule. In the additive case, the watermark is added to a set of image features, such as grey level pixels or frequency coefficients [14]. In the non-additive watermarking, depending on the host characteristics, the embedding process is performed which results in better robustness and transparency [15]. Multiplicative watermarking methods are well-known examples of non-additive data hiding methods.

In this paper, we introduce a video watermarking technique which is highly robust to video-based attacks. To insert watermark, the scaling based rule proposed in [2, 3] has been used for low frequency components of 3-D video blocks. Considering the distribution of the watermarked approximation coefficients, we use maximum likelihood (ML) decoder for data extraction. We make some assumption on the embedding parameter and the channel noise to simplify the detection process, leading us to a real-time decoding scheme. Embedding in the low frequency components of video signals, as well as optimal detection, makes our algorithm to be quite robust against attacks.

The rest of the paper is organized as follows. In section 2 we introduce the embedding and detection parts of our watermarking scheme. Performance of the proposed method is analyzed in section 3. Section 4 shows the experimental results and section 5 concludes the paper.

2. PROPOSED SCHEME

2.1 Watermark embedding

For data embedding, we first segment the video signals into non-overlapping 3-D blocks. The format of the video signal is assumed to be AVI (Audio Video Interleave). To this aim, each frame which is in fact an image is segmented into $B \times B$ non-overlapping blocks. Then, over every T consecutive frames, we obtain $B \times B \times T$ blocks. This procedure is performed until the entire video signal is divided into non-overlapping blocks which are taken as the carriers in our watermarking system. To have better transparency, we may

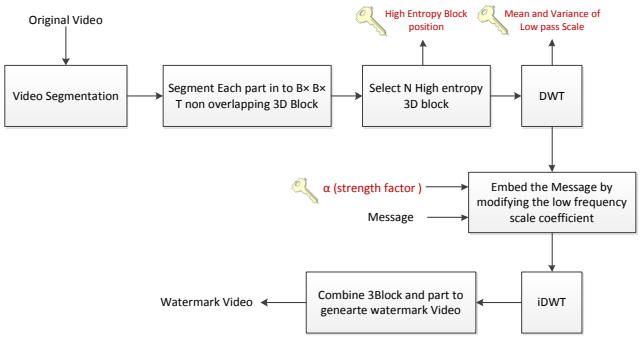

Figure 1: Block diagram of the proposed watermarking decoding scheme

choose blocks with the most entropy to which eye is less sensitive according to human visual system (HVS) model [16].

For robustness against attacks, the best places for data hiding are the low frequency components, where the least variations are allowed in case of the compression or filtering attack. However, these components are very sensitive to any modifications that make the watermark invisibility quite challenging. In our system, taking the advantage of wavelet transform, we decompose each 3D block into different subbands and approximation coefficients are used for data embedding. If we denote these *LLL* approximation coefficients with U_i, the embedding process is performed using the following scaling based rule [2]:

$$U_i' = U_i.\alpha \qquad M_i = 0 \quad , \quad U_i' = U_i.\frac{1}{\alpha} \qquad M_i = 1 \qquad (1)$$

In (1), the parameter α is called the strength factor which controls the power of watermark. By adjusting this parameter properly, the blocking effect is under control and thus the watermark would be transparent [3]. In fact, α makes a trade-off between the quality of the watermarked signal and its robustness against attacks. Fig 1 demonstrates the block diagram of the proposed data embedding scheme.

2.2 Watermark detection

In the decoder, the same procedure should be done. First, we segment the received video into the 3D blocks. Then, by applying the 3D wavelet transform, the watermarked approximation coefficients are computed. In order to detect the message bit, we use the optimal ML decoder. To this end, we need the distribution of watermarked approximation coefficients of the 3D video blocks. Mihcak, et al. show that the wavelet coefficients of images can be modeled as a Gaussian process [17]. Besides, using Kolmogrov-Smirnov test, Akhaee et al [2] demonstrate the approximation coefficients of image blocks can be well-modeled by an i.i.d Gaussian distribution. Therefore, since we work on the AVI signals that contain consecutive images, the same model is applicable.

Suppose we denote the approximation coefficients of video blocks as U_i with mean μ and variance σ^2. After transmitting the signal over the channel, the watermarked signal might be contaminated with additive white Gaussian noise (AWGN). Since the channel noise is Gaussian and uncorrelated to the watermarked signal, the received signal remains Gaussian with the following distribution:

$$W_i|0 = \alpha.U_i + n_i \quad \Rightarrow \quad W_i|0 \backsim \mathcal{N}(\alpha\mu_{|0}, \sigma^2_{W|0}) \qquad (2)$$

$$W_i|1 = \alpha^{-1}.U_i + n_i \quad \Rightarrow \quad W_i|1 \backsim \mathcal{N}(\alpha^{-1}\mu_{|1}, \sigma^2_{W|1}) \qquad (3)$$

In these equations $\sigma^2_{W|0} = \alpha^2\sigma^2 + \sigma^2_n$ and $\sigma^2_{W|1} = \alpha^{-2}\sigma^2 + \sigma^2_n$. Besides, $\mu_{|1} = \alpha^{-1}\mu$ and $\mu_{|0} = \alpha\mu$. These parameters must be known to the decoder. We should send some of these parameters as side information along with the watermarked signal, while some other parameters like the noise variance should be estimated. Since we have applied the wavelet transform, it is rational to use the technique proposed by *Donoho* [18] based on the detail coefficients. To do this, the noise variance is estimated by applying a median filter to detail (HH) coefficients of the image, as:

$$\hat{\sigma} = \frac{Median(|W_i|)}{0.6745} \qquad W_i \in subbandHH \qquad (4)$$

We estimate the noise variance in the subband in which our decoder is employed. As a consequence, the standard deviation of the noise in the *LL* subband can be computed by multiplication of the norm of the *LL* filter impulse response as:

$$\sigma_n = \| L \| \hat{\sigma} \qquad \sqrt{\Sigma_l \Sigma_k L^2(l,k)} \qquad (5)$$

The distribution of N approximation coefficients of video blocks after embedding the bit 0 or 1 can be calculated as:

$$P(W_1,\ldots,W_N|0) = \prod_{i=1}^{N} \frac{1}{\sqrt{2\pi\sigma^2_{W|0}}}.e^{-(W_i-\alpha\mu_{|0})^2/2.\sigma^2_{W|0}}$$

$$P(W_1,\ldots,W_N|1) = \prod_{i=1}^{N} \frac{1}{\sqrt{2\pi\sigma^2_{W|1}}}.e^{-(W_i-\alpha^{-1}\mu_{|1})^2/2.\sigma^2_{W|1}} \qquad (6)$$

For date extraction, we use the ML rule as:

$$P(W_1,W_2,\ldots,W_N|0) \gtrless_1^0 P(W_1,W_2,\ldots,W_N|1) \qquad (7)$$

Substituting (6) in (7), we have:

$$\prod_{i=1}^{N} \frac{1}{\sqrt{2\pi\sigma^2_{W|0}}}.e^{-(W_i-\alpha^2\mu)^2/2.\sigma^2_{W|0}} \gtrless_1^0$$

$$\prod_{i=1}^{N} \frac{1}{\sqrt{2\pi\sigma^2_{W|1}}}.e^{-(W_i-\alpha^{-2}\mu)^2/2.\sigma^2_{W|1}} \qquad (8)$$

By applying logarithmic function to both sides and doing some simplifications, (8) can be written as:

$$(\frac{1}{\sigma^2_{W|1}} - \frac{1}{\sigma^2_{W|0}}) \sum_{i=1}^{N} W_i^2 - 2\mu(\frac{\alpha^{-2}}{\sigma^2_{W|1}} - \frac{\alpha^2}{\sigma^2_{W|0}}) \sum_{i=1}^{N} W_i \gtrless_1^0$$

$$2N\ln(\frac{\sigma_{W|0}}{\sigma_{W|1}}) - N\mu^2(\frac{\alpha^{-4}}{\sigma^2_{W|1}} - \frac{\alpha^4}{\sigma^2_{W|0}}) \qquad (9)$$

For the case where the variance of the noise is far smaller than the variance of the video block, which usually happens, (9) can be further simplified as:

$$(\alpha^4 - 1)(\Sigma_{i=1}^{N} W_i^2 - N\mu^2) \gtrless_1^0 4N\alpha^2\sigma^2\ln(\alpha) \qquad (10)$$

Transparency of the watermark limits the value of α to be near one. Thus, by denoting $\alpha = 1+\varepsilon$ which ε has a small value, equation (10) can be written as:

$$\Sigma_{i=1}^{N} W_i^2 \gtrless_1^0 N(\sigma^2+\mu^2) = N \times E\{U^2\} \qquad (11)$$

According to (11), the proposed detector is independent of the strength factor in low noisy environment. In addition, there is no need for sending both mean and variance of each block separately. The value of $\sigma^2+\mu^2$, which is in fact the second moment of the *LLL* coefficients, is enough to be sent through a secure channel.

3. PERFORMANCE ANALYSIS

Here, we drive the error probability of the proposed watermarking technique at the presence of the AWGN. The error occurs whenever the bit one is embedded in an image block while zero is decoded at the receiver end and vice versa. Without loss of generality, suppose one is embedded. According to (9), the error happens when:

$$\begin{aligned} P_{e|0} &= P\left(A\sum_{i=1}^{N} W_i^2 + B\sum_{i=1}^{N} W_i < C|0\right) \qquad (12)\\ A &= \frac{1}{\sigma_{W|1}^2} - \frac{1}{\sigma_{W|0}^2} \quad B = -2\mu\left(\frac{\alpha^{-2}}{\sigma_{W|1}^2} - \frac{\alpha^2}{\sigma_{W|0}^2}\right)\\ C &= 2N\ln\left(\frac{\sigma_{W|0}}{\sigma_{W|1}}\right) - N\mu^2\left(\frac{\alpha^{-4}}{\sigma_{W|1}^2} - \frac{\alpha^4}{\sigma_{W|0}^2}\right) \end{aligned}$$

Suppose $X_i = \frac{W_i - \alpha\mu}{\sigma_{W|1}}$. According to (2), $W_{|1}$ has a Gaussian distribution, so $X_i \sim N(0,1)$ has a normal distribution.

$$\sum_{i=1}^{N} W_i^2 = \sigma_{W|1}^2 \sum_{i=1}^{N} X_i^2 + 2\alpha\mu\sigma_{W|1}\sum_{i=1}^{N} X_i + N(\alpha\mu)^2 \qquad (13)$$

We define $\Omega_N = \sum_{i=1}^{N} X_i^2$ and $\Phi_N = \sum_{i=1}^{N} X_i$. Since X_i has a normal distribution, Ω_N will have a chi-square distribution, and Φ_N comes with a normal distribution. By substituting (13) in (12) and after some simplification, we have:

$$\begin{aligned} P_{e|0} &= P\left(a\Omega_N + b\Phi_N < c'\right) \qquad (14)\\ a &= A\sigma_{W|1}^2 \quad b = \sigma_{W|1}(2A\alpha\mu + B) \quad c' = c - N(\alpha\mu)^2 \end{aligned}$$

Suppose $f_{\Omega_N}(x)$ and $f_{\Phi_N}(x)$ are probability density functions and $F_{\Omega_N}(x)$ and $F_{\Phi_N}(x)$ are their cumulative distribution functions respectively. As mentioned earlier, Ω_N has a Chi-square distribution $\chi^2(N)$, and Φ_N has has a normal distribution $\Phi_N \backsim \mathcal{N}(0,N)$. We can now calculate $P_{e|0}$ as follows:

$$\begin{aligned} P_{e|0} &= \int_{-\infty}^{\infty} f_{\Omega_N}(x)\left(\int_{-\infty}^{\frac{c'-ax}{b}} f_{\Phi_N}(y)\mathrm{d}y\right)\mathrm{d}x\\ P_{e|0} &= \int_{0}^{\infty} f_{\Omega_N}(x) F_{\Phi_N}\left(\frac{c'-ax}{b}\right)\mathrm{d}x \qquad (15) \end{aligned}$$

If we use integration by parts, (15) can be rewritten as:

$$\begin{aligned} P_{e|0} &= \left[F_{\Omega_N}(x)F_{\Phi_N}\left(\frac{c'-ax}{b}\right)\right]_0^{\infty}\\ &+ \frac{1}{\sqrt{2N\pi}}\cdot\frac{a}{b}\int_0^{\infty} F_{\Omega_N}(x) e^{-\frac{\left(\frac{c'-ax}{b}\right)^2}{2N}}\mathrm{d}x \qquad (16) \end{aligned}$$

where in (16), cumulative distribution function for Ω_N can be written as [19]:

$$F_{\Omega_N} = \mathscr{P}\left(\frac{N}{2}, \frac{x}{2}\right) \qquad (17)$$

In above equation, $\mathscr{P}(k,x)$ is the regularized Gamma function. Therefore, the error probability of zero embedding is:

$$P_{e|0} = \frac{1}{\sqrt{2N\pi}}\cdot\frac{a}{b}\int_0^{\infty} \mathscr{P}\left(\frac{N}{2},\frac{x}{2}\right) e^{-\frac{\left(\frac{c'-ax}{b}\right)^2}{2N}}\mathrm{d}x$$

Similar approach can be taken to compute $P_{e|1}$. For the case of the bit 1 embedding, we have:

$$P_{e|1} = 1 - \frac{1}{\sqrt{2N\pi}}\cdot\frac{a'}{b'}\int_0^{\infty} \mathscr{P}\left(\frac{N}{2},\frac{x}{2}\right) e^{-\frac{\left(\frac{c''-a'x}{b'}\right)^2}{2N}}\mathrm{d}x$$

Total error can be computed as:

$$\begin{aligned} P_e &= P_{e|0} + P_{e|1} = 1 + \frac{1}{\sqrt{2N\pi}}\int_0^{\infty} \mathscr{P}\left(\frac{N}{2},\frac{x}{2}\right)\\ &\left[\frac{a}{b}e^{-\frac{\left(\frac{c'-ax}{b}\right)^2}{2N}} - \frac{a'}{b'}e^{-\frac{\left(\frac{c''-a'x}{b'}\right)^2}{2N}}\right]\mathrm{d}x \qquad (18) \end{aligned}$$

4. EXPERIMENT RESULT

In this section, experimental results are shown. We have used various video signals, in the AVI format, to evaluate the performance of the proposed method. 3D wavelet coefficients are achieved after three levels of decomposition using a Daubechies filter of length 4. The message is embedded into the approximation coefficients (*LLL*). We use *Hollywood2* for our experiments [20].

The quality of the watermarked signal is measured using Peak Signal to Noise ratio (*PSNR*). Error probability is calculated as the ratio of number of error bits to the total number of watermark bits transmitted through the channel.

4.1 Change in block size and message length

As the first experiment, we show the role of message length through changing the 3D block size. Three types of attack, the AWGN with the standard deviation of 30, median filtering (3×3 window), and Wiener filtering (5×5 window) are examined here. We just use a part of the total capacity (*Cap*), which is calculated by dividing the total number of pixels of video signal to the 3-D blocks of size $B\times B\times B$. Table 1 shows the average results for 65 video signals while α is fixed to 1.015 . As shown, the best performance (capacity, robustness, and transparency) is achieved when the block size is $16\times16\times16$. This block size is used for the rest of our simulations.

4.2 The effect of α

In order to investigate the effect of watermark power on the robustness, we have changed the value of α. The white noise with standard deviation of 30 is taken as an attack to 16 frames of each video signal. The results are shown in Table 2 for average of 100 video signals. The total number of watermarked bits is $.5\times Cap$ for each video. As expected, by increasing α, higher robustness against noise is achieved at the expense of lower quality of the watermarked signal.

Table 1: The effects of block size and the message length

	$8\times8\times8$				$16\times16\times16$				$32\times32\times32$			
$\frac{MessageLength}{Cap}$	PSNR	Noise	Wiener	Median	PSNR	Noise	Wiener	Median	PSNR	Noise	Wiener	Median
0.2	54.08	23.07	18.34	14.05	53.82	5.40	5.12	7.56	54.16	0.51	0.80	6.03
0.3	52.77	24.52	19.76	13.13	52.54	7.28	6.03	7.16	52.74	0.48	1.64	6.33
0.4	51.88	25.55	19.70	12.21	51.68	7.90	7.11	6.58	51.84	1.00	1.83	5.96
0.5	51.23	26.93	20.82	11.15	51.06	9.01	7.60	6.15	51.20	1.49	2.38	5.95
0.6	50.70	27.24	20.58	10.63	50.60	10.17	8.12	5.73	50.73	1.46	3.14	6.60
0.7	50.30	28.08	20.46	9.88	50.22	11.13	8.77	5.54	50.34	2.22	3.09	5.89
0.8	49.97	28.82	20.10	9.25	49.90	12.09	8.77	5.26	50.02	2.51	3.50	5.51
0.9	49.69	29.24	19.24	8.68	49.63	13.00	8.77	4.99	49.75	3.77	4.01	5.87
1.0	49.47	29.91	18.80	8.52	49.39	14.03	8.85	4.83	49.48	4.81	4.34	5.42

Table 3: BER (%) after the noise attack

σ	4	10	16	22	28	34	40
BER (%) for Gaussian noise	0.07	1.00	2.89	5.13	7.55	10.07	12.55
BER (%) for uniform noise	0.00	0.00	0.00	0.30	0.80	1.00	1.51

Table 2: The effect of α on the quality and robustness

α	1.007	1.013	1.016	1.019	1.022	1.028
PSNR	58.84	53.49	51.70	50.22	48.96	46.89
BER (%)	18.02	8.85	6.72	5.39	4.20	2.89

Table 4: The robustness against Gaussian Filter attack with different parameters

σ	3×3	5×5	7×7
0.2	0	0	0
0.4	0	0	0
0.6	0.377	0.353	0.419
0.8	1.57	2.32	2.46
1.0	2.17	4.88	5.39

Table 5: Bit error rates of Median, mean and Wiener filter attack

Filter Type	3×3	5×5	7×7
Median Filter	1.11	7.57	15.59
Mean Filter	0.43	6.49	16.02
Wiener Filter	4.87	14.43	20.50

Table 6: BER (%) after the Motion Filtering Attack

$\theta(degree)$	2	6	10	14
BER (%)	4.38	4.33	4.66	4.67

Table 7: Result of M-JPEG compression attack

Quality Factor	10	20	30	40	50	60
BER (%)	17.41	6.14	2.60	1.20	0.49	0.42

4.3 Noise attack

In this experiment, Gaussian noise and uniform noise with zero mean and different standard deviations, are added to the watermarked signal. The mean results of 77 video signals are shown in Table 3. As shown, the proposed method is highly robust against noise attack. This is due to using optimal decoder as well as embedding watermark in the low frequency components of the host signal. We fix the value of α to 1.015 which guarantees the transparency while keeping the performance at an acceptable level. The length of the embedded message is $.5\times Cap$ for each video signal.

4.4 Filtering attacks

The resistance of our method to several filtering attack is investigated here. In this experiment, we use 80 video signal. For median, Wiener and Mean filtering, the results are shown for several window sizes, i.e. 3×3, 5×5, 7×7 in Table 5. In Table 4, the error probability is demonstrated following Gaussian filtering with different window sizes and sigma values. In the video camera, if the shutter speed is too slow and the camera is in motion, a given pixel will be an amalgam of intensities from points along the line of the camera's motion. Blurring due to a linear motion in the photograph is the result of poor sampling. We can model the linear motion of the camera by a filter with two parameters (length in pixels and angle θ in degrees). We applied the Motion filter of the length 3 and different θs to each frame of the video signal. Table 6 reports the results of this motion filter attack versus θ. We can see that the proposed method is highly robust against these five processing attacks. This is due to the fact that watermark has been inserted in the approximation coefficients.

4.5 M-JPEG compression attack

Motion JPEG (M-JPEG) is a class of video formats where each video frame is separately compressed with JPEG compression. M-JPEG is now used by many portable devices with video-capture capability, such as digital cameras. We embedded $.5\times Capacity$ message bit in each 75 video signal, and then compressed them with M-JPEG. Finally, we extracted the message bits at the receiver side, after decompressing each video signal. Table 7 shows the message error versus different JPEG quality factors.

Table 8: Result of MPEG compression attack

α	1.015	1.016	1.017	1.019	1.020	1.021
BER(%)	11.13	7.22	3.90	0.59	0	0

4.6 MPEG compression attack

As the last part of our experiments, we show the robustness of our watermarking method against the MPEG compression attack that might happen before transmission to reduce the cost/time of this process. At the receiver, first, the reverse process, converting the MPEG to the AVI format, is performed and then the data extraction is done. In Table 8, the results obtained at different strength factors (α) are shown. As observed, an acceptable performance is achieved if the watermark power is selected appropriately.

5. CONCLUSION

We have presented a multiplicative watermarking scheme suitable for video signals in the AVI format. The embedding is performed by slightly modification of approximation coefficients, subband corresponding to *LLL*, of 3D video blocks. By modeling the modified noisy coefficients with the Gaussian distribution, we implement an ML decoder for data extraction. Simulation results show that the suggested technique is highly robust against different attacks. The MPEG transmission of the watermarked video is possible by simply converting the watermarked AVI signal into the MPEG format. However, as a future work, we are trying to embed the watermark in a compressed format directly, so that we would be able to reduce the complexity cost of the system.

REFERENCES

[1] G. Doërr, "A Guide Tour of Video Watermarking," *Signal Processing: Image Communication*, vol. 18, pp. 263–282, Apr. 2003.

[2] M. A. Akhaee, S. M. E. Sahraeian, B. Sankur, and F. Marvasti, "Robust Scaling-Based Image Watermarking Using Maximum-Likelihood Decoder With Optimum Strength Factor," *IEEE Transactions on Multimedia*, vol. 11, pp. 822–833, Aug. 2009.

[3] M. Akhaee, N. Khademi Kalantari, and F. Marvasti, "Robust Audio and Speech Watermarking Using Gaussian and Laplacian Modeling," *Signal Processing*, vol. 90, pp. 2487–2497, Aug. 2010.

[4] Y. Chen and H. Huang, "A New Shot-Based Video Watermarking," in *Computer Communication Control and Automation (3CA), International Symposium on*, vol. 2, pp. 53–58, IEEE, 2010.

[5] M. Belhaj, M. Mitrea, F. Preteux, and S. Duta, "MPEG-4 AVC robust video watermarking based on QIM and perceptual masking," in *Communications (COMM), 8th International Conference on*, pp. 477–480, IEEE, 2010.

[6] G. Langelaar, R. Lagendijk, and J. Biemond, "Real-Time Labeling of MPEG-2 Compressed Video," *Journal of Visual Communication and Image Representation*, vol. 9, no. 4, pp. 256–270, 1998.

[7] R. Lancini, F. Mapelli, and S. Tubaro, "A Robust Video Watermarking Technique In the Spatial Domain," in *Video/Image Processing and Multimedia Communications 4th EURASIP-IEEE Region 8 International Symposium on VIPromCom*, no. June, pp. 251–256, IEEE, 2002.

[8] B. Mobasseri, "Direct Sequence Watermarking of Digital Video Using M-Frames," in *Proceedings International Conference on Image Processing (ICIP-98)*, vol. 2, pp. 399–403, IEEE, 1998.

[9] S. a. M. Al-Taweel and P. Sumari, "Robust Video Watermarking Based On 3D-DWT Domain," in *TENCON , IEEE Region 10 Conference*, pp. 1–6, Ieee, Nov. 2010.

[10] F. Deguillaume, G. Csurka, J. O'Ruanaidh, and T. Pun, "Robust 3D DFT Video Watermarking," in *Proceedings of IS&T/SPIE Electronic Imaging*, vol. 3657, pp. 113–124, Spie, 1999.

[11] M. Swanson and A. Tewfik, "Multiresolution Scene-Based Video Watermarking Using Perceptual Models," *IEEE Journal on Selected Areas in Communications*, vol. 16, pp. 540–550, May 2002.

[12] P. Chan and M. Lyu, "A DWT-Based Digital Video Watermarking Scheme With Error Correcting Code," in *Proceedings of Fifth International Conference on Information and Communications Security*, pp. 202–213, Springer, 2003.

[13] X. Guo-juan and W. Rang-ding, "A Blind Video Watermarking Algorithm Resisting to Rotation Attack," *International Conference on Computer and Communications Security*, pp. 111–114, Dec. 2009.

[14] R. C. Motwani, M. C. Motwani, B. D. Bryant, F. C. Harris Jr., and A. S. Agarwal, "Watermark Embedder Optimization for 3D Mesh Objects Using Classification Based Approach," *International Conference on Signal Acquisition and Processing*, pp. 125–129, Feb. 2010.

[15] I. Cox, J. Kilian, F. Leighton, and T. Shamoon, "Secure Spread Spectrum Watermarking For Multimedia," *Image Processing, IEEE Transactions on*, vol. 6, no. 12, pp. 1673–1687, 2002.

[16] a. B. Watson, G. Y. Yang, J. a. Solomon, and J. Villasenor, "Visibility of Wavelet Quantization Noise," *IEEE transactions on image processing : a publication of the IEEE Signal Processing Society*, vol. 6, pp. 1164–75, Aug. 1997.

[17] K. Mihcak, I. Kozintsev, K. Ramchandran, and P. Moulin, "Low-Complexity Image Denoising Based On Statistical Modeling of Wavelet Coefficients," *Signal Processing Letters, IEEE*, vol. 6, no. 12, pp. 300–303, 1999.

[18] D. Donoho and J. Johnstone, "Ideal Spatial Adaptation By Wavelet Shrinkage," *Biometrika*, vol. 81, no. 3, p. 425, 1994.

[19] M. R. Spiegel, J. J. Schiller, and R. A. Srinivasan, *PROBABILITY AND STATISTICS BASED ON SCHAUM S Outline*. McGraw-Hill Professional, 2002.

[20] [Online], "[Available] http://www.irisa.fr/vista/actions/hollywood2."